Journal of the Korean Society for Nondestructive Testing
Vol. 29, No. 6 (2009. 12)

Detection of Second-Layer Corrosion in Aging Aircraft

Nohyu Kim*† and Seunyong Yang**

Abstract The Compton backscatter technique has been applied to lap-joint in aircraft structure in order to determine mass loss due to exfoliative corrosion of the aluminum alloy sheet skin. The mass loss of each layer has been estimated from Compton backscatter A-scan including the aluminum sheet, the corrosion layer, and the sealant. A Compton backscattering imaging system has been also developed to obtain a cross-sectional profile of corroded lap-splices of aging aircraft using a specially designed slit-type camera. The camera is to focus on a small scattering volume inside the material from which the backscattered photons are collected by a collimated scintillator detector for interpretation of material characteristics. The cross section of the layered structure is scanned by moving the scattering volume through the thickness direction of the specimen. The theoretical model of the Compton scattering based on Boltzmann transport theory is presented for quantitative characterization of exfoliative corrosion through deconvolution procedure using a nonlinear least-square error minimization method. It produces practical information such as location and width of planar corrosion in layered structures of aircraft, which generally cannot be detected by conventional NDE techniques such as the ultrasonic method.

Keywords: Compton Scattering, Digital X-ray, Aging Aircraft, Corrosion

1. Introduction

A typical form of corrosion occurring often in aluminum aircraft structures is exfoliative(or layered) corrosion. Exfoliation is a term used to describe a type of corrosion which takes place parallel to the metal surface. When this occurs, flakes of metal peel or are pushed from the surface due to internal stresses caused by the building up of corrosion products. It is most common in rolled or extruded aluminum alloy products(Al-Cu-Mg and Al-Zn-Mg) such as the aluminum skin in aircraft in which grains are elongated and flattened. Exfoliative corrosion in rolled aluminum alloy sheet appears as “mass loss” or “thinning” of the aluminum skin in aging aircraft, and it may subsequently lead to a structural failure. A special characteristic of exfoliative corrosion in aluminum is porosity which allows the corrosion to grow in the direction in which the aluminum alloy plate has been re-crystalized in the rolling process. This fact is supported by SEM(scanning electron micrograph) of samples of aircraft corrosion products which show them to be porous by an amount of near 50 percent. This porosity is a main contributor to low electron density, which is proportional to the physical density for a low atomic number material. This is a distinguishing characteristic of exfoliative corrosion in aging aircraft which is used for corrosion detection by the Compton backscattering technique. Once the

Received: November 16, 2009, Revised: December 11, 2009, Accepted: December 14, 2009. *Department of Mechatronic Engineering, Korea University of Technology and Education, 307 Gajun-Ri, Byungchun-Myun, Chunan 330-860, Korea, **Department of Mechanical Engineering, Korea University of Technology and Education, Byungchun-Myun, Chunan 330-860, Korea, †Corresponding Author: nykim@kut.ac.kr

exfoliative corrosion proceeds in the inner layer of the layered structure, the corrosion products tend to separate from the skin surface, so that the total effective thickness of the skin becomes smaller, which weakens the structural strength of the aircraft. Experimental results of fatigue test indicate that the average life is not affected for a slightly exfoliated material but is reduced more than 50 percent for a severely exfoliated material. That is, the existence of even a small amount of exfoliation can initiate a fatigue crack. Corrosion is usually found on the entire aircraft after a long period of operation, although most of it is benign. However, it must be watched and inspected constantly. A little metal loss less than 10% is tolerable for the skins of most commercial aircraft. But over 10%, the loss significantly weakens the structure especially when it is combined with crack propagation in the structure(Lawson, 1993). The parts most susceptible to the corrosion in aging aircraft are honeycomb assemblies and fuselages because they provide an easy path and spare for moisture to enter and be trapped inside for a longer time than in other parts. Also water in honeycomb core or lap-joint of fuselage can freeze and expand, subsequently causing failure of the aluminum skin itself or of the adhesive bond line between aluminum skin and the honeycomb core. Honeycomb is not of interest in this study because it does not have a layered structure like a lap joint of fuselage. The main concern of this study is focused on the corrosion of fuselage multi-layered structures of aging aircraft.

In this paper, a detailed assessment of mass loss due to exfoliative corrosion in aging aircraft structures is made by constructing a true cross-sectional view of layered structure such as a lap-joint of aircraft fuselage structure using a specially designed Compton backscattering imaging system for aircraft inspection. A mobile X-ray backscatter system is developed for the purpose, and applied to inspect a number of locations of possibly severe corrosion along a lap splice on a Boeing 737 testbed. Data processing and reconstruction for deconvolution is carried out to determine the mass loss of each layer of the lap splice.

2. NDT Methods for Detection of Layered Corrosion in Aging Aircraft

A variety of NDT methods have been tried for the purpose of measuring metal loss due to corrosion(Lawson and Kim, 1994). The most common and easy inspection technique is visual inspection. The corrosion product in the first skin layer of a fuselage structure shows a swelling made by porosity and corrosion products, so that they can be detected usually. This inspection is clearly valuable, but one cannot expect to detect the forms of corrosion that may be present beyond the first skin layer in a lap-joint. Furthermore, if damage is detected, it is important that other tools be used to assess the extent of the corrosion because subsurface damage may be difficult to access quantitatively. One technique which has potential to evaluate aircraft corrosion is the eddy current method. This method works well for measuring the first layer of metal but the sensitivity drops rapidly with depth due to the skin effect. Ultrasonic methods have many advantages for providing one-sided measurements of layered joints, but they require continuity of the structure all the way through because a small air gap blocks the transmission of ultrasonic waves. Air gaps are very common between layers in older aircraft, and even a small air gap blocks ultrasound. Thermal wave imaging is a technique which produces a thermal pattern by thermal waves and can be used to monitor the surface of the part for relatively hot spots caused by blockage of thermal flow away from the surface by a laminar flaw. This method is very sensitive to flaws near the inspection surface but the sensitivity reduces rapidly with flaw depth. Like thermal wave imaging, shearography, a laser holographic technique, can rapidly scan large

areas of aircraft skin. Even though it does not have the vibration problems of conventional interferometric holography, it is limited to the detection of defects or disbonds near the surface.

Traditional transmission X-ray inspection which has been frequently applied for detection of corrosion uses transmitted radiation for imaging purposes and it provide a good image for the corroded area. It is very useful for the detection of honeycomb-core defect in bonded sandwich assemblies. True 3-D information can be obtained at the cost of a significant increase in system complexity, by viewing the object from many different directions, and manipulating the set of projections to reconstruct in some way the spatial distribution of the linear attenuation coefficient(computer tomography). It is, however, very limited in real in-situ inspection because the structure should be accessible from both sides, which is generally impossible for airplanes.

Compton backscattering permits the placing of the source and the detector on the same side of the object. It provides indications of material-density changes by a change in intensity slope .vs. position and of voids or foreign material by an abrupt change in backscatter intensity. This method is particularly useful for the inspection of laminated structures. For some of these layered structures, ultrasonic inspection approaches are ineffective or impractical, but the backscatter X-ray technique offers a solution. The backscatter technique can be particularly useful as a complementary quantitative inspection to a fast imaging method. For radiographically thin material(where the product of the attenuation coefficient and material thickness is less than one), Compton backscatter imaging technique competes in sensitivity with transmission techniques(Harding and Kosanetzky, 1989).

3. Compton Scattering of X-ray in Material

The total interaction of photons with material in the range of energy for many industrial inspections(typically 50-200 KeV) is composed of Compton scatter, photoelectric absorption, and coherent Rayleigh scatter(Bessi et al., 1988). The scattering of X-ray photons back toward the source is mainly made by Compton scattering. In the Compton interaction of a photon with an electron, the electron is considered to be free if its initial binding energy is small compared to the incident photon energy E. Therefore each electron makes its independent contribution to the total scattering, which is thus proportional to the number of electrons per volume, ρ_ε(electron density). In the absence of other effects in the radiation scattered from different electrons, the cross section per unit volume is the product of the scattering cross section per electron and the electron density ρ_ε. Thus there is usually good correlation between the electron density and the physical density of a sample. This fact that Compton scattering is proportional to the electron density has stimulated much work both in the medical and industrial fields. After the incident photon of energy E collides with the free electrons, they will recoil and have energy E' which is given by(Fernandez, 1989)

$$E' = \frac{m_o c^2}{1-\cos\theta + (m_o c^2/E)} \tag{1}$$

Where, θ is the scatter angle for the photon and m_0c^2=511 keV. The energy of the scattered photon is a function of the scattering angle and the initial energy. Around 100-150 keV, the backscattered(90-180 degrees) energy is a much larger fraction of the initial energy than at higher keV(1 MeV). The probability of scattering in a particular direction is given by the differential cross section(σ) per unit solid angle (Ω) for collisions. This is based on the Klein-Nishina equation, which is given by

$$\frac{d\sigma}{d\Omega} = \eta \left(\frac{E'}{E}\right)^2 \left(\frac{E}{E'} + \frac{E'}{E} - \sin^2\theta\right) \tag{2}$$

where η is a proportionality factor. The Klein-Nishina formula describes the variation of the intensity of the scattered photons as a function of the scattering angle θ. This equation shows that the backscatting(90-180 degrees) is not as great as the forward scatter(0-90 degrees) but is of useful intensity. A practical consequence of this characteristic is the possibility of one-sided inspection of bulky objects like airplane surfaces, oil pipes and so on.

4. Narrow Beam Model for Compton Scattering Field

Suppose a very well-collimated narrow beam of intensity I_0 is directed to a point, the origin of the z-x coordinate system with an incident angle of θ_0 as shown in Fig. 1(a). The mathematical model of Fig. 1(a) is illustrated in Fig. 1(b) where a point source placed at the origin propagates a ray in the direction of angle θ_0 with the intensity I_0. Defining f(z,X,ω,λ as the flux at point (z,x) into the direction of ω with the wavelength λ in the 2-dimensional z-x plane the Boltzmann transport equation of photon flux in the material is expressed by (Mackcormick, 1992; Kim 2000)

$$\omega\cdot\nabla f(z,x,\omega,\lambda) = -\mu(\lambda)f(z,x,\omega,\lambda) + \iint k(\omega,\lambda,\omega',\lambda')H(z)f(z,x,\omega',\lambda')d\omega'd\lambda' + I_0\delta(z)\delta(x)\delta(\omega-\theta_0)\delta(\lambda-\lambda_0) \quad (3)$$

Where, H(z) is heavy side function and $k(\omega,\lambda,\omega',\lambda')$ is the probability function of Compton scattering associated with the famous Klein-Nishina differential coefficient.

Now if we consider the primary beam, i.e., the zero-th scattering solution $f^{(0)}(z,x,\omega,\lambda)$(primary X-ray), the governing equation eqn. (3) is simplified by deleting the scattering term from the equation (3) to yield

$$\omega\cdot\nabla f^{(0)}(z,x,\omega,\lambda) = -\mu(\lambda)f^{(0)}(z,x,\omega,\lambda) + I_0\delta(z)\delta(x)\delta(\omega-\theta_0)\delta(\lambda-\lambda_0) \quad (4)$$

Since the zero-th scattering always occurs only along the line of the incident source beam which is shown by the dashed line in Fig. 1(b), the solution of eqn. (4) can be found as(Kim, 2000)

$$f^{(0)}(z,x,\omega,\lambda) = \frac{I_0}{2}\delta(z-\cot(\theta_0)x)\delta(\omega-\theta_0)\delta(\lambda-\lambda_0)(1+\mathrm{sgn}(z))e^{-\mu\left|\frac{z}{\cot(\theta_0)}\right|} \quad (5)$$

This equation describes the zero-th order flux at an arbitrary point (z, x) into the direction of ω and the wavelength $\tilde{\lambda}$. For higher order scattering, for example, the n-th scattering field in 2-dimensional half-space shown in Fig. 2, the source term in the Boltzmann equation of eqn. (4) drops out, and the equation becomes

$$\omega\cdot\nabla f^{(n)}(z,x,\omega,\lambda) = -\mu(\lambda)f^{(n)}(z,x,\omega,\lambda) + \iint k(\omega,\lambda,\omega',\lambda')H(z)f^{(n-1)}(z,x,\omega',\lambda')d\omega'd\lambda' \quad (6)$$

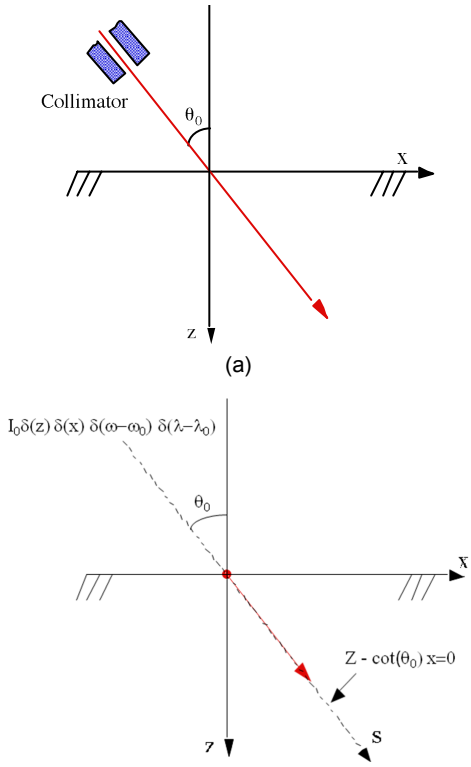

Fig. 1 Narrow beam model, (a) physical model, (b) mathematical model

In Fig. 2, the scattering direction ω is the propagation vector of the scattering photon, while ω_0 the propagation vector of the incident photon.

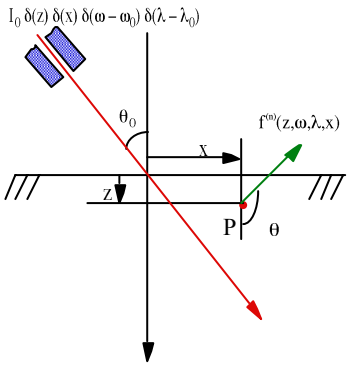

Fig. 2 Narrow beam model for multiple scattering

If only the first-order scattering, the most dominant contributor to the total scattering flux, is considered, it can be obtained as

$$f^{(1)}(z,\omega,\lambda,x)=\frac{I_0 k(\omega,\lambda,\omega_0,\lambda_0)}{4}\exp\left[-\frac{\mu\,|-G(\theta)\,\gamma\cos(\theta)|}{|\eta^{(0)}|}\right]$$

$$[1+\mathrm{sgn}(-G(\theta)\,\gamma\cos(\theta))]\cdot\exp[-|z\cos(\theta)+G(\theta)\,\gamma|\,\mu]$$

$$[1-\mathrm{sgn}(-z\cos(\theta)-G(\theta)\,\gamma)] \qquad (7)$$

$$\text{where, } \gamma = z-\cot(\theta)\,x,\ G(\theta)=\frac{\cot(\theta_0)\tan(\theta)}{\cos(\theta)-\sin(\theta)\cot(\theta_0)},$$

$$\text{and } \eta^{(0)}=\cos(\theta_0)$$

Equations (6) and (7) are very important in applications to practical nondestructive inspection or evaluation. First of all, they give an explicit mathematical expression for the single scattering flux in the direction of θ at arbitrary point in a solid, when a narrow incident beam illuminates the solid under an arbitrary angle $\tilde{\theta}_0$. These equations can be used in a computer simulation to obtain a theoretical backscattered signal from a certain point of interest inside a material. In addition, these explicit equations provide a basic tool for designing or optimizing the backscattering system in terms of balancing the resolution and the flux of the system. They also make it possible to calculate the multiple scattering(double scattering) effect on the total scattering flux. This effect should be taken into account when inspecting a radiographically thick material.

5. Compton Backscattering System

X-ray backscattering method is a digital imaging technique that gives a true cross-sectional view of the object being examined unlike conventional radiographic techniques which are shadow-casting techniques. Because it is based on backscattering rather than transmission, it can perform inspections of aircraft structures from the outside of the plane without needing access to the interior. X-ray backscattering system(XBS) has been developed to provide a highly accurate depth profile in a location of interest. XBS eliminates the costly labor and time needed for rivet removal required for direct measurement with calipers. XBS gives that additional information about thickness which is needed in order to make the decision of whether or not repairs are needed and how soon.

To collect backscatter data for corrosion evaluation, the depth-profiling camera, shown in Fig. 3, was developed. The camera consists of a radiation detector and sets of precision apertures for accurate collimation. One pair of apertures along with the focal spot of X-ray tube defines the source collimation. A second such pair defines the detector's field of view. The first forms the beam into a pencil with a narrow rectangular cross-section. The second pair of apertures selects a limited-thickness region from

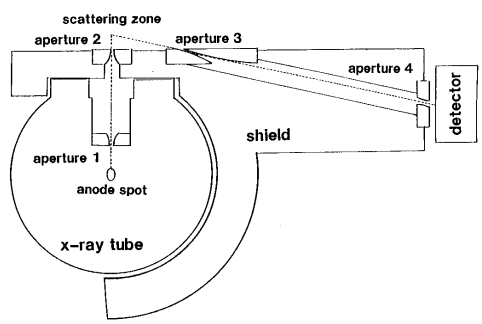

Fig. 3 3 Compton backscatter camera of XBS

which backscattered photons reach the detector. Backscattered photons from the selected scattering zone fall upon a thallium-doped sodium iodide scintillation detector placed outside aperture.

The intersection of the incident and backscattered beam pencils forms the selected scattering zone. Sweeping this scattering zone through the material to be examined allows visualization along the swept path of the electron density of the material. For aluminum and lighter elements the electron density is equal to a constant times their mass density. The camera is mounted on a camera head assembly to scan it in a direction perpendicular to the surface being examined. In Fig. 4(a), the configuration of entire inspection system is described schematically, where the camera assembly moves in thickness direction with help of stepping motor through computer. The XBS assembly designed for field test is represented in Fig. 4(b).

A-scan data of Compton scattering system may be thought of as being like a density scan plot of a sample core-drilled through the skin. The term "virtual core drill" has been used to describe the XBS machine for this reason. The resolution of the XBS system has been adjusted to measure the thickness of the layers of aircraft skin with an accuracy of about 25 μm. This is near to the best accuracy obtainable when measuring the thickness of metal which has not been polished.

6. Inspection of Corroded Fuselage in Aging Aircraft.

The XBS apparatus was taken to airport hangar for validation test. Fig. 5 shows the XBS being used to inspect a station along a lap splice on a Boeing 737 aircraft located at the hangar facility. The XBS unit moves around under its own battery power. The unit is positioned at the point where the scan is to take place, and the scan head is guided to the exact location by an operator. The operator controls the boom and can pivot the scan head. When the scan head is in place, its four foots shown in Fig 4(b) rest against the plane's surface. Then by operating the boom, the spring-loaded scan head is pressed against the plane. Friction of the feet against the surface holds the scan head in place. The boom supports the scan head(camera) and simultaneously applies pressure to the scan head's feet in whatever position the head may be placed. Fig. 5(a) shows the scan head in position against the side of the plane. Fig. 5(b) shows the scan head rotated and lifted for inspection of the belly section. Once in place, the scan head is precisely re-aligned by computer-controlled stepper motors using position sensors which contact the plane and then the scan begins. The computer performs the scan, advancing the motors and stopping at intervals to collect data.

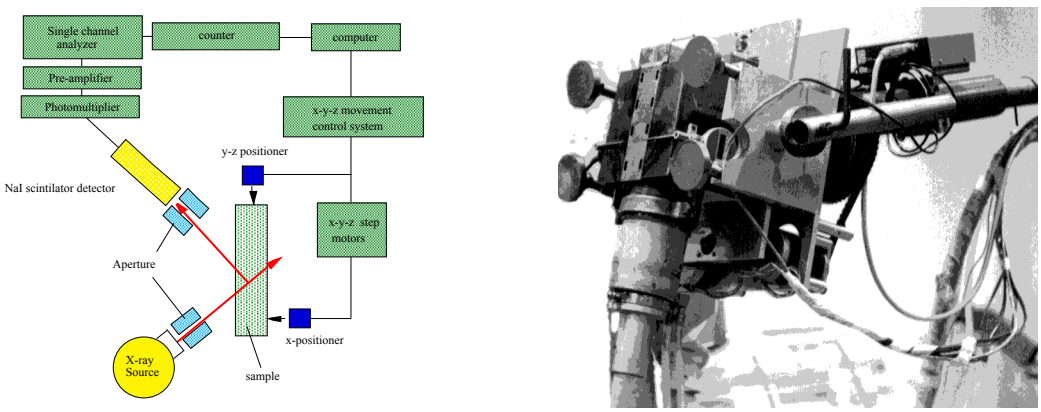

(a) (b)

Fig. 4 X-ray backscattering system, (a) configuration of XBS, (b) assembled system

These intervals are usually 25 μm. During the scanning, the computer rechecks alignment and realigns the scan head as needed. If the backscatter signal drops below a certain value, the computer interrupts the scan and queries the operator for instructions. The indications, in a scan, of unexpected low-density material, air gaps and thinning of metal, are the hallmarks of corrosion in an aircraft sheet metal joint. The presence of loose low density material signals active or untreated corrosion. Air gaps alone, unless greater than hundreds of micron in width, do not by themselves indicate corrosion. But they do provide good places for corrosion to start and seem to be present in very many if not all joints in older aircraft. Corrosion products, when compacted, often appear in a scan as material having about half the density of the parent aluminum. Loose corrosion products often have still lower densities.

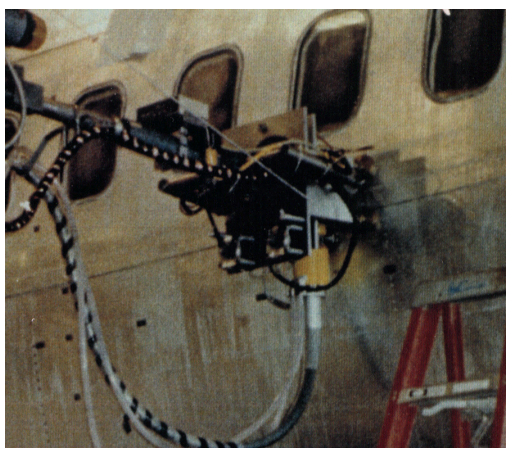

(a)

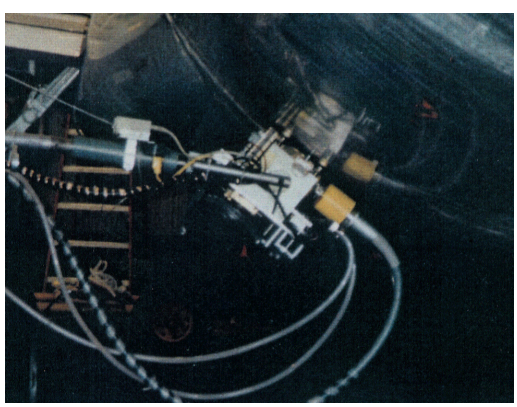

(b)

Fig. 5 Inspection of B-737 testbed fuselage, (a) side section, (b) belly part

The lap-splice of the B-737 testbed fuselage shown in Fig. 5 is composed of three layers, which are the outer skin, the inner skin, and a hat channel as shown in Fig. 6. The outer and inner skins are polished and riveted together to the hat channel. A doubler, a faying strip or a sealant is often inserted either between the two skins or behind the inner skin in order to prevent propagation of fatigue cracks and corrosion. Hence, the scan images taken from different spots on a lap-joint may show two or three, sometimes four/five layers depending on the scan point on the lap-joint. Fig. 6 shows that typical scan points are in one of the two regions of the lap-joint, one of which is the region A where only two skins can be seen with or without a sealant or a doubler between them. The other one is the region B where a structural element such as a stringer or a longeron is detected behind the two aluminum sheets.

Fig. 7(a) displays raw scan data taken from a lap joint at a point like A region in Fig. 6, which shows large attenuation in each layer. Its reconstructed image is Fig. 7(b), where the attenuation in each layer is compensated so well that each layer has a flat-top shape.

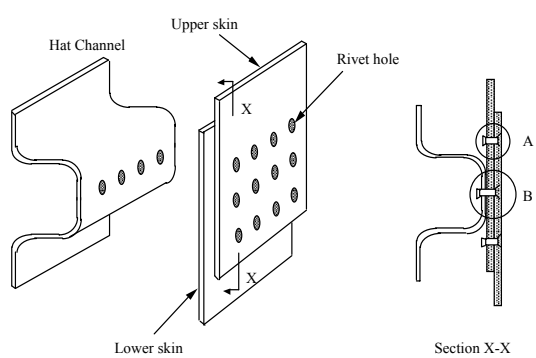

Fig. 6 Lap joint of the B-737 testbed fuselage

7. Deconvolution and Restoration of Compton Backscatter Data

After the scan over the surface of fuselage, the next step for the characterization of corrosion is to calculate the thickness and location of corrosion and aluminum layers from the A-scan data, which is called as deconvolution procedure. While convolution is associated with the forward problem of generating the response of a system from known values of its input and impulse response function(IRF) of the system, deconvolution is associated with the inverse problem of determining the input to the system from known values of output and IRF. However, it is not really possible to obtain the operation IRF^{-1} simply by inverting a system's impulse response function except for very rare cases, because the inversion of the system's IRF becomes very unstable when zeros of the system lie outside of the unit circle in the complex z-domain. Additionally the measured output of the system is usually corrupted by noise. Therefore, a deconvolution based on deterministic principles is generally inadequate. Instead, a deconvolution based on stochastic principles can handle both effects. The stochastic approach used in this paper for solving the inverse problem combines and compares measurement result with mathematical solutions of the direct problem obtained for different values of the unknowns, which are here the thicknesses of layers. For the case of M data points, we can define a least-square functional Φ as flux difference between the measured flux $F^m(z_j)$ and theoretically expected flux $F^c(z_j)$at a scan position z_j. In stochastic approach, the solution of the inverse problem is obtained by minimizing the value of the functional Φ. In this study, the functional is defined as

$$\Phi = \frac{1}{2}\sum_{j=1}^{M}[F^c(z_j) - F^m(z_j)]^2 \tag{8}$$

From eqn. (8), the solution of the inverse problem is obtained by minimizing the value of the functional Φ. The scan data obtained between rivets at several points of the lap-splice have been processed through this deconvolution after reconstruction to obtain the thickness and location of each layer.

In Fig. 8(a), this deconvolution procedure is described in detail. The dotted line in the Fig. 8(a) is a reconstructed data obtained from the region A in Fig. 7, where only two aluminum sheets appear, but between them exists a low density material which may be a bonding resin or a corrosion product. The solid line in Fig. 8(b) represents the curve-fitting result of reconstructed

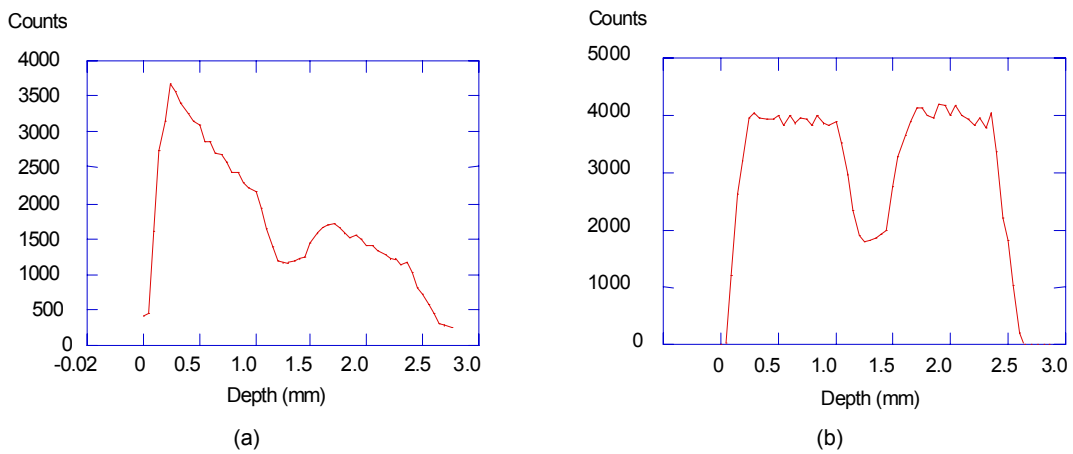

Fig. 7 Reconstruction of raw data, (a) raw data obtained from a lap-joint of the B-373 testbed, (b) reconstructed data

data(dotted line) using the previously described stochastic method(nonlinear minimization method in eqn. (8)). In Fig. 8(b) where a low density material is assumed between the two skins, the restored data (solid line) very well fits over the whole range. Therefore, it may be concluded that the low density material is a resin bond or a corrosion product trapped between the skins, or both of them. Through the nonlinear minimization algorithm in computer, the thickness of each layer is calculated and its results are displayed in diagram in Fig. 8(c) and 8(d).

Fig. 9 is another scan taken at a region A with a faying strip or sealant between the two aluminum skins. In Fig. 9(a), there are clear disbonds between the aluminum skin and the faying layer which strongly imply the development of corrosion inside the gap. The back surface of the lower aluminum skin seems to be painted because the slope of the dotted curve at the back surface in Fig. 9(a) is a little bit lower than that of the curve-fitted line(solid). After the deconvolution process described previously, the thickness of each layer is clearly seen and obtained easily in Fig. 9(b).

The scan in Fig. 10 was conducted in the same manner in the region B where three layers were detected. The first and second skin in Fig. 10 is partly detached from both skins leaving a air gap which probably indicates the presence of corrosion. The rear surface of the second skin is not bonded well either. Each layer is separated and filled with a low density material, which is not exfoliative corrosion, but simply air gap in this case. The third layer is an aluminum doubler with 0.711 mm in thickness. Visual

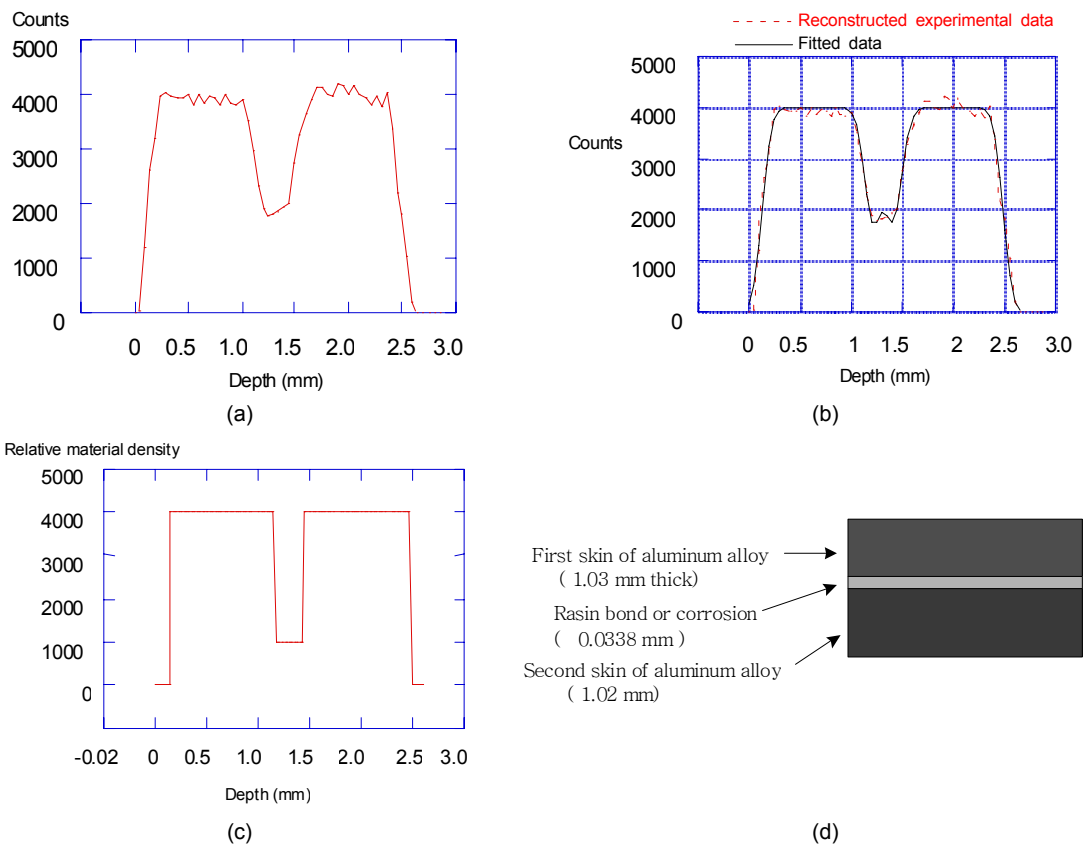

Fig. 8 Reconstruction and deconvolution of scan data in region A, (a) reconstructed data, (b) reconstructed data and curve-fitted data by optimization method when the second layer is assumed as a low density material, (c) restored data, (d) thicknesses of layers

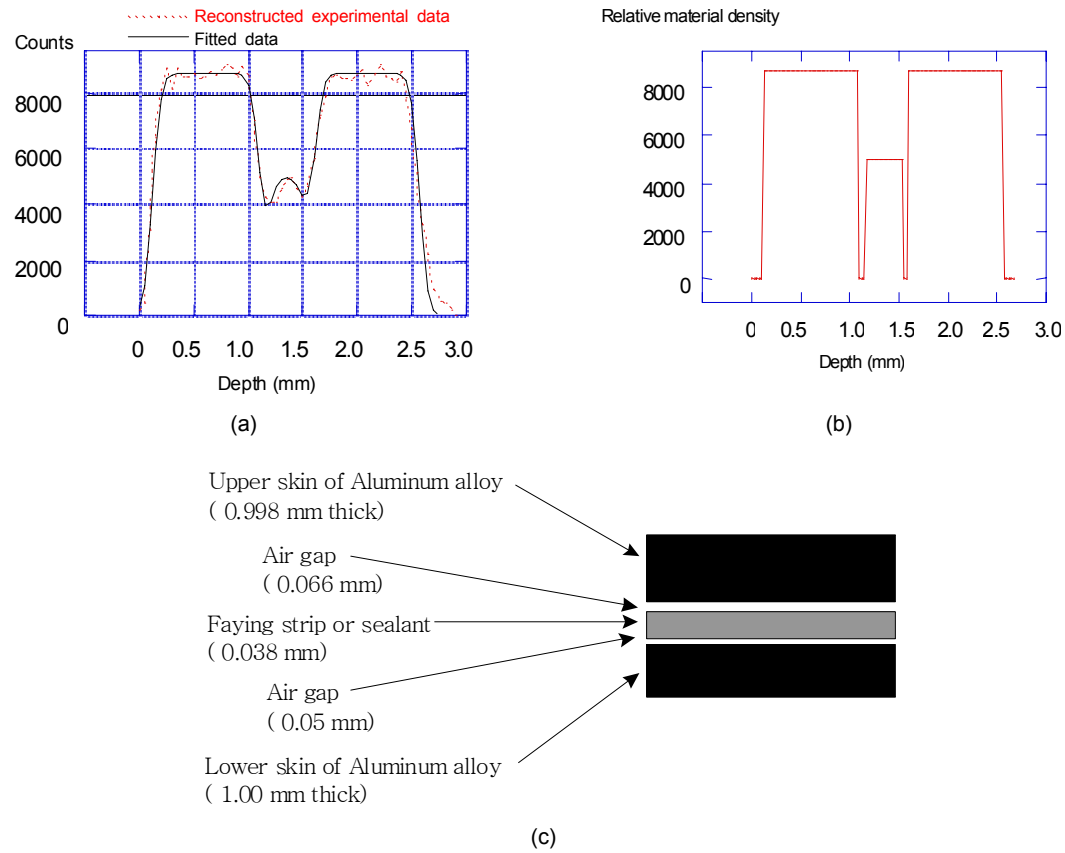

Fig. 9 Data processing and deconvolution of scan data from a lap-joint in region A, (a) reconstructed data and curve-fitted data, (b) deconvolved data, (c) thicknesses of layers.

inspection inside the Boeing 737 testbed showed that the doubler was indeed this thick at points near where the scan was taken.

8. Conclusions

This study was devoted to the development of Compton backscattering technique to characterize second or third layer corrosion in layered aluminum structures of aging aircrafts. Such defects are generally difficult to detect by other methods. Layered corrosion was assumed to be planar and parallel to the surface of the structure, so that the 3-dimensional Boltzmann equation reduced to two-dimensional equation. The two dimensional Boltzmann equation was derived and solved for a homogeneous half space to analyze single and multiple scattering. Unlike the Monte Carlo approach, it has a great flexibility for parametric studies to optimize the performance of the imaging system. The Compton backscattering imaging system is proved in experiment at field test to be suitable for high resolution inspection of a radiographically thin structure like aluminum skins of aircrafts. From the theoretical and experimental results performed in this study, the following conclusions can be made.

1. X-ray backscattering imaging system is designed to provide a highly accurate depth profile at a location of interest(about 25 micron)
2. This technique can detect damage to the second layer or interface debonding, and thereby give evidence of corrosion activity.

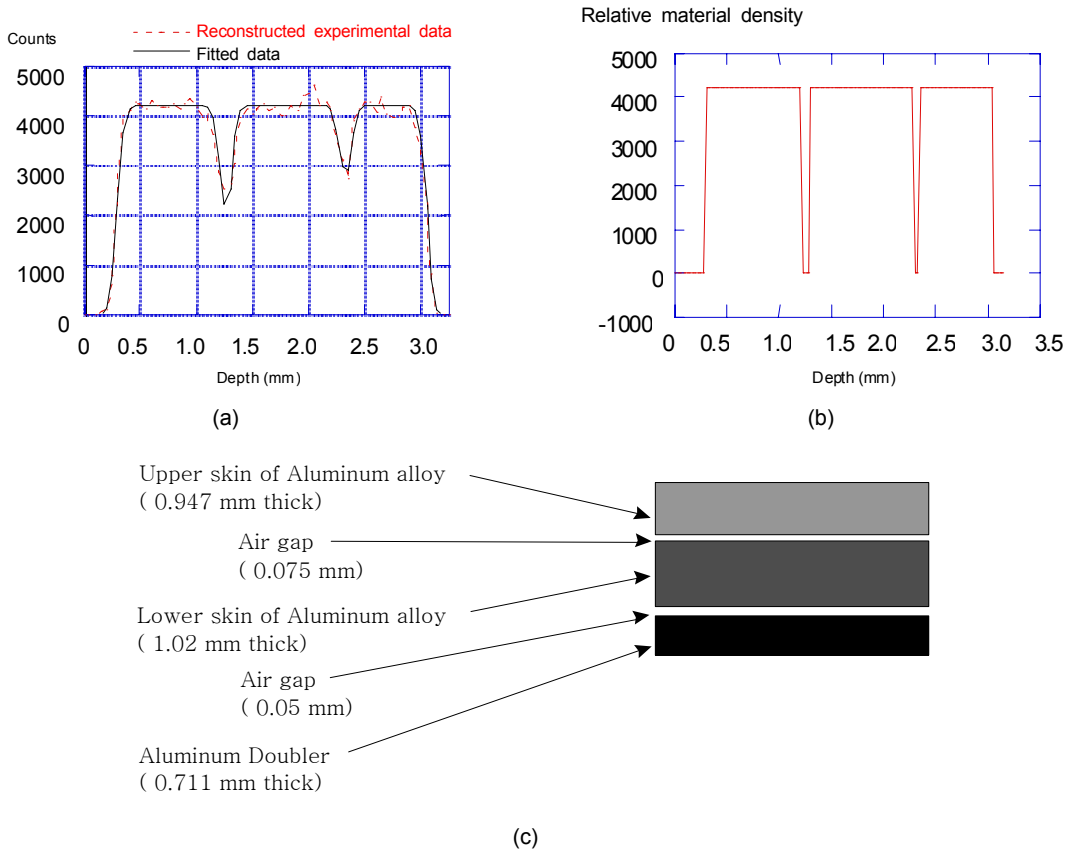

Fig. 10 Data processing and deconvolution of scan data from a lap-joint in region B, (a) reconstructed data and curve-fitted data, (b) deconvolved data, (c) thicknesses of layers

3. X-ray system gives additional information about thickness which is needed in order to make decision of whether or not repairs are needed and how soon.
4. X-ray backscattering Technique makes possible a non-contact one-sided inspection and does not require the continuity in the material.
5. XBS eliminates the costly tear-down time needed for rivet removal required for direct measurement with calipers

Acknowledgments

This work was supported by the Korea Science and Engineering Foundation(KOSEF) grant funded by the Korea government (MEST).

References

Bessi, H., Friddell, K. D. and Nelson, J. M. (1988) Backscatter X-ray Imaging, *Materials Evaluation*, Vol. 46, pp. 1462-1468

Fernandez, Jorge E. (1989) XRF Intensity in the Frame of the Transport Theory, *Nuclear Instruments and Methods of Physical Research*, A 280, pp. 212-221

Harding, G. and Kosanetzky, J. (1989) Scattered X-ray Beam Nondestructive Testing, *Nuclear Instruments and Methods*. A280, pp. 517-521

Harding, G. (1982) On the Sensitivity and Application Possibilities of a Novel Compton

Scatter Imaging System, *IEEE Transaction on Nuclear Science*, Vol. NS-29, No. 3, pp. 178-184

Kim, Nohyu (2000) Reconstruction and Deconvolution of X-ray Backscatter Data Using Adaptive Filter, *Journal of the Korean Society for Nondestructive Testing*, Vol. 20, No. 6, pp. 1-9

Lawson, L. (1993) Measurement of Layered Corrosion with Compton Backscatter, in: D. O. Thompson and D. E. Chimenti, (Eds.), *Review of Progress in Quantitative Non-Destructive Evaluation*, Plenum, NY., Vol. 12b, pp 1971-1978

Lawson, L. and Kim, N. (1994) Deconvolution and Detectability in Compton Backscatter Profilometry, in: D. O. Thompson and D. E. Chimenti, (Eds.), *Review of Progress in Quantitative Non-Destructive Evaluation*, Plenum, NY., Vol. 13b, pp 1971-1978

Mackcormick, J. (1992) Inverse Radiative Transfer Problems : A Review, *Nuclear science and Engineering*, Vol. 112, pp. 185-198